Dynamic Design Considerations for an Impulsed-Corrected, Laser-Guided Rocket

Kenneth K. Cobb*
Air Force Armament Laboratory, Eglin Air Force Base, Fla.

An analysis of the dynamics and accuracy of a laser-guided fin-stabilized rocket has been conducted. A quadrant detector, body-fixed guidance is used without gyroscopic or relative wind reference. Corrections are made using short action time impulses located forward of the mass center. Simulations are used to show the effects of several phenomena on the accuracy of this type of system. Some of these phenomena are the relation between the laser pulse frequency and rocket angular motion, the relation between trim misalignment, pitch frequency, and roll rate, and the maximum expected correction as a function of rocket system parameters. Equations and curves are presented which show these relationships. The study shows that, for the phenomena considered, accuracy is controllable through parameter selection.

Nomenclature

cal = calibers, diam
C_x = axial drag (thrust off)
$C_{N\alpha}$ = normal force coefficient derivative
$C_{m\alpha}$ = restoring moment coefficient derivative
C_{mq} = damping moment coefficient derivative
$C_{m\dot{\alpha}}$ = damping moment coefficient derivative
$C_{\dot{\phi}\delta}$ = spin driving moment coefficient
$C_{\dot{\phi}p}$ = spin damping moment coefficient
d = missile reference diameter
$\bar{F}_S$ = average constant side force
f = $\rho sd/2M$
I_x, I_y = axial transverse inertia moments
I_{xr}, I_{yr} = gyration radii
K_t = dynamic trim misalignment angle
$-L$ = forward distance, c.g. to thruster center
M = missile mass
M_b = missile mass at burnout
m = depleted thrusters at impact minus one
N = number of thrusters
p = spin rate
Q = dynamic pressure = $\rho V^2/2$
q = pitch rate
R_0 = distance to impact at guidance initiation
$\bar{R}$ = distance to mean point of impact of random trajectory trials to target
R_t = $\bar{R} + \sigma_{cep}$
s = missile reference area
t = time from launch
t_2 = time from side thrust termination
T = axial thrust
T_ℓ = period between laser pulses
T_f = guided flight time
V = velocity of the rocket
$\bar{V}$ = average rocket velocity during guidance = R_0/T_f
X = downrange distance
$\dot{X}$ = X component of velocity of c.g.
$X_{c.g.}$ = distance of velocity of c.g.
$\dot{Z}$ = Z component of velocity of c.g.
$\alpha(t_2)$ = missile angle of attack at time t_2
$\dot{\alpha}$ = angle-of-attack rate
α_p = the particular constant in the differential equation solution for α_τ
α_τ = missile angle of attack at side thrust termination τ
$\dot{\alpha}_\tau$ = missile angle-of-attack rate at τ
δ_s = change in velocity vector direction due to side thrust, rad
$\Delta\bar{X}_{ep}, \Delta\bar{Y}_e$ = mean point of impact in plane perpendicular to trajectory
δ_{rp} = maximum correction toward target
δ_{rpq} = maximum correction quadrant detector
δ_m = static trim misalignment angle (trim angle at zero spin)
ρ = air density (average)
σ_{cep} = bivariate 50% circle radius
τ = side thrust termination time
ω_l = pitch frequency for planar motion

Presented as Paper 77-1139 at the AIAA 4th Atmospheric Flight Mechanics Conference, Hollywood, Fla., Aug. 8-10, 1977; submitted Oct. 17, 1977; revision received March 7, 1978.

Index categories: LV/M Dynamics and Control; LV/M Aerodynamics; LV/M Simulation.

*Physicist. Member AIAA.

Introduction

THE system being considered is a pulsed laser-guided fin-stabilized rocket, which makes guidance correction by means of short action time discrete impulses located forward of the center of mass. The corrections are made when the periodic laser pulse reflections from the target are received. (See Fig. 1a for a pictoral view of a hypothetical missile.) The rocket has no instrumentation indicating the angle of attack, and any angle of attack (including angles of attack induced by the correction impulses) will result in incorrect signals to the quadrant corrector guidance system. The pulsed laser image reflected from the target is received in one of the four quadrants, indicating that the longitudinal axis of the missile is not in line with the target. The seeker logic then initiates one of the discrete impulses (action time approximately 10^{-4} s) in the image quadrant. The impulse units are expended in a predetermined sequence. In this manner, the velocity vector (to the extent that the angle of attack is small when the correction is made) is turned in line with the target. Part of the correction comes from motion of the c.g. due to the linear momentum impulse, and the remainder comes from the lift force generated by the angle of attack which is induced primarily by the moment of the impulse.

The advantages of the type of guidance being considered are that it is simple and inexpensive. The guidance package contains no gyros or other moving parts. The following phenomena can affect the accuracy or effectiveness of this

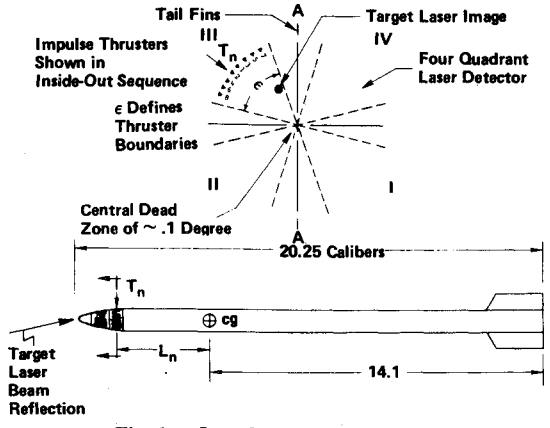

Fig. 1a Impulse control geometry.

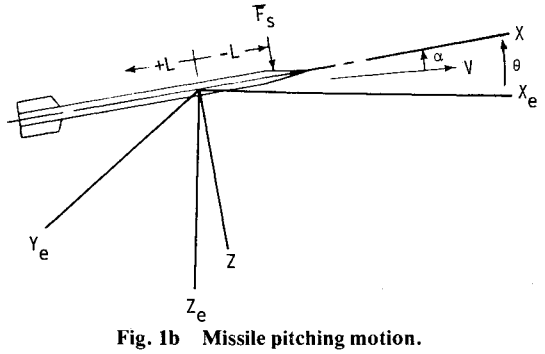

Fig. 1b Missile pitching motion.

body-fixed system adversely, and an understanding of them is essential in developing the system:

1) There is a limited correction from the discrete impulses determined by their number, magnitude, and interaction with the aerodynamic and physical properties of the rocket.

2) The rocket angle of attack at correction will be interpreted incorrectly by the seeker as an error in the direction of the velocity vector. The angle of attack may result from the impulse corrections themselves or a trim misalignment of the rocket.

This paper considers the maximum expected correction as a function of the rocket system parameters; the relation between the laser pulse frequency, the pitch frequency, and missile accuracy; and the relation between the static trim misalignment, the pitch frequency, the roll rate, and the missile accuracy. A more complete analysis of this type of system, including gravity sag, target motion and wind, and disturbed flow effects, is given in Refs. 1 and 2.

In studying the guidance system, it is necessary to simulate the motion of the rocket, the logic and correction of the guidance system, and all associated errors. Two simulation computer programs are used in this study. The first is a simple closed-form solution to the pitching motion which is used in analyzing the pitching frequency, angle of attack, and magnitude of the impulse correction. The second computer program is a complete six-degree-of-freedom program, which models the entire guidance system. This includes physical and aerodynamic properties of the rocket, the guidance logic, the force and moment of the impulse corrections, atmospheric conditions, and target motion.

Linear Pitching and Swerve Motion

The linear equations of motion for a rolling missile are described in many publications, including Ref. 3. For the slow roll rates considered here (10 to 20 Hz), the nutation is only about 1% greater than the precession frequency. The frequncy for pure pitching motion will be between these two frequencies. Then, for the more complicated case of motion induced by side impulse, the planar motion solution will give most of the information required to understand the motion.

For the impulse guidance being considered, it is important to understand the relationship between the motion of the rocket after side impulse and all of the parameters affecting the motion. The differential equations for the angular and swerving motion for the planar case were set up from Fig. 1b. These differential equations are derived in exactly the same way as in Ref. 3, with the exception of the additional force and moment term due to the side thrust ($\bar{F}_s$, $\bar{F}_s L$). These equations were solved using small-angle approximations, eliminating terms of small magnitude, and assuming steady-state conditions (velocity and spin).[1] The quantities of importance – the angle of attack $\alpha(t_2)$, the pitch frequency ω_I, and the side deflection or swerve δ_s – were derived in this manner and are listed below:

$$\alpha(t_2) = \exp(\lambda t_2)\left[\alpha_\tau \cos\omega_I t_2 + \left(\frac{\dot{\alpha}_\tau}{\omega_I} - \frac{K_{\dot{\alpha}}\alpha_\tau}{2\omega_I}\right)\sin\omega_I t_2\right] \quad (1)$$

$$\alpha_\tau = \alpha_p\left[\exp(\lambda t_2)\left(-\cos\omega_I\tau + \frac{K_{\dot{\alpha}}}{2\omega_I}\sin\omega_I\tau\right) + 1\right] \quad (2)$$

$$\dot{\alpha}_\tau = \alpha_p\omega_I\exp(\lambda t_2)\sin\omega_I\tau\left[1 + \left(\frac{K_{\dot{\alpha}}}{2\omega_I}\right)^2\right],\ \lambda = \frac{K_{\dot{\alpha}}}{2} \quad (3)$$

$$\alpha_p = \frac{-\bar{F}_s L}{K_\alpha I_y} + \frac{\bar{F}_s C_{mq} d}{2MV^2 C_{m\alpha}} \quad (4)$$

$$\omega_I = \sqrt{-K_\alpha - K_{\dot{\alpha}}^2/4)} \quad (5)$$

$$K_\alpha = \frac{\rho V^2 \pi d^3 C_{m\alpha}}{8I_y},\ K_{\dot{\alpha}} = \rho\pi d^4 V\frac{(C_{mq} + C_{m\dot{\alpha}})}{16I_y} \quad (6)$$

$$\delta_s = \frac{-fV}{d}C_{N\alpha}\alpha_p\left[\exp(\lambda t_2)\frac{K_{\dot{\alpha}}{}^2}{4K_\alpha\omega_I}\sin\omega_I\tau + 2\tau\right] + \frac{\bar{F}_s\tau}{MV} \quad (7)$$

In order to visualize the relationship between the parameters of the rocket system, a hypothetical baseline configuration was selected using the approximate shape given in Fig. 1a. This configuration is tabulated in Tables 1-3 and was used along with preceding equations to show the relationship among some of the parameters.

In Fig. 2, the maximum angle of attack α_m, obtained from Eq. (1), is plotted as it varies with normalized total impulse (thruster impulse/rocket average momentum $= \bar{F}_s\tau/M\bar{V}$). It is

Table 1 Baseline configuration physical characteristics[a]

t, s	M/Mb, normalized mass	Gyration radius, cal I_{xr}	I_{yr}	c.g., cal-base
0	1.41	0.483	5.39	11.7
2.0	1.00	0.527	5.06	14.1
2.1	Guidance commence		20/s	Laser pulse frequency,

[a] Axial specific impulse = 240 lb-s/(lb-mass propellant); $-L = 4.35$ calibers forward of c.g.

Table 2 Primary aerodynamic characteristics[4]

Mach	C_x	C_{n_α}	C_p, cal-base	C_{m_α}	C_{mq}	$C_{l\delta}$	C_{lp}
2.0	0.49	11.00	5.37	−95.8	−4110	0.075	−6.4
2.5	0.41	9.40	6.03	−75.8	−3540	0.052	−6.3
3.0	0.34	8.59	6.90	−61.8	−3320	0.035	−6.0
3.5	0.31	7.96	7.86	−49.7	−3160	0.015	−3.9

Table 3 Performance[a]

			30-deg dive				
t, s	Alt, ft	X, ft	Slant range, ft	V, ft/s	$\dot{X}$, ft/s	$\dot{Z}$, ft/s	Dive angle, deg
0.0	6000	0	11310	760	658	380	30.0
2.0	3946	3372	7358	3282	2788	1733	31.9
2.1	3774	3651	7031	3266	2772	1726	31.9
4.4	0	9583	0	2855	2393	1558	33.1

[a] Average spin during guidance ~ 14.1 rps.

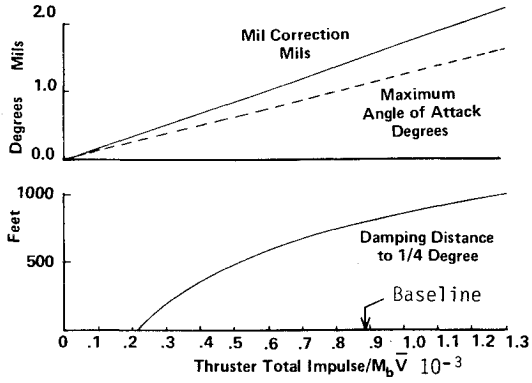

Fig. 2 Mil correction, angle of attack, and distance to damp vs thruster normalized total impulse.

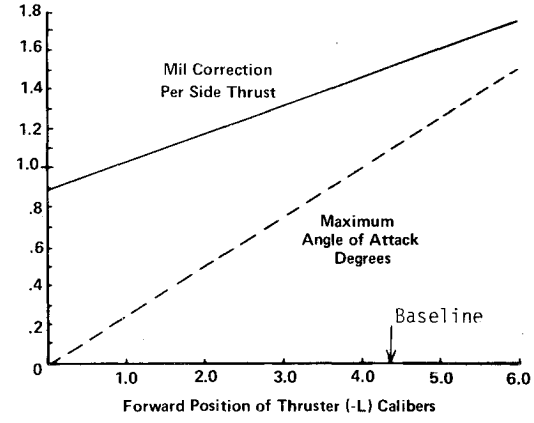

Fig. 3 Correction vs thruster position.

desired to keep the angle as small as feasible. The milliradian change in the velocity vector per impulse thrust, [δ_s Eq. (7)], as it varies with the thruster impulse, also is plotted. This value should be large to obtain large side corrections.

The distance that the rocket must move before the maximum angle of attack damps to 0.25 deg also is plotted in Fig. 2. The 0.25 deg was selected since it is necessary to have the angle of attack this small in order to obtain sufficient accuracy. The plot was made using Eq. (1). For reasonable impulses (0.0007 and above), the distance to damp to 0.25 deg would be greater than 700 ft. This means that we cannot rely on damping to have a small angle of attack when corrections are made.

Figure 3 gives the mil correction and maximum angle of attack for the baseline configuration plotted vs the distance of the thrust center forward of the c.g. location. The plot shows that the maximum angle of attack is extremely small, ~0.005 deg, if the side thrust is located at the center of gravity ($L = 0$). The mil correction for this thrust location is 0.888 mil. This is about 59% of the nominal value (1.50 mils), corresponding to the center of thrust located 4.48 cal forward of the c.g. Because of the smaller angle of attack, the guidance system is more accurate for the thrust center close to the c.g. The angle of attack, the mil correction, and simplicity of design must be considered in the design.

Relation between the Laser Pulse Frequency and Pitch Frequency

The angle of attack of the missile must be relatively small when a correction is made, since the angle of attack is interpreted as an error in the velocity vector direction. As shown, there is not sufficient damping between laser pulses to reduce the angle of attack to acceptable values. The method used to overcome this problem is to have the missile pitch frequency (essentially the same as nutation and precession frequency for slow roll) slightly larger than one-half the laser pulse frequency (LPF). Under these conditions, the angle of attack is small when a correction is made, and the impulse tends to oppose the angular motion.

The foregoing can be understood qualitatively from Fig. 4. Figure 4 shows planar motion; however, for the fast impulse system being considered, the six-degree-of-freedom motion is nearly planar. A correction is made toward the target, where the initial velocity vector is V_1. The angle of attack moves to α_{1m} and swings back through the zero-angle-of-attack position, since the pitch frequency is a little over one-half the LPF. The second correction is made when the angle of attack is $\alpha_{2\ell}$, and the correction $\bar{F}_2$ is generally in the opposite direction of the angular velocity. This tends to cause the random error corrections to be out of phase with the angular velocity and prevents a resonant buildup of angle of attack. If the pitch frequency were less than ½ LPF, a resonant buildup of the angle of attack would occur, and the accuracy would be reduced greatly. This is demonstrated clearly from the six-degree-of-freedom output given below.

Six-degree-of-freedom trajectories were run using the rocket configuration given in Tables 1-3 and a target array characteristic of the nonguided accuracy of this rocket. Different pitch frequencies were obtained by varying the c.g. location of this configuration. Figure 5 gives the angle-of-attack history for two pitch frequencies, and Fig. 6 was generated by using the target array for 12 different pitch frequencies.

In Fig. 5, the upper curve is for the frequency of 10.3 Hz (above resonance), and the lower curve is for a frequency of 9.78 Hz in the resonant region. It is obvious that for the 9.78 pitch frequency the maximum angle of attack is building up and is up to about 2.0 deg at 2.86 s. (The plot covers only about one-third of the guided flight.) The plot show that the average angle of attack at lase time also is building up.

The effect of the angle of attack and resonant condition on guided accuracy is shown in Fig. 6. The distance from target to mean point of impact and CEP[5] values are plotted vs the pitch frequency. The angle of attack is plotted to illustrate the relationship between resonance angle of attack and guided accuracy for this system.

Approximate Maximum Expected Correction

In the system being considered, the corrections toward the target are a result of the thrust impulse units, which are

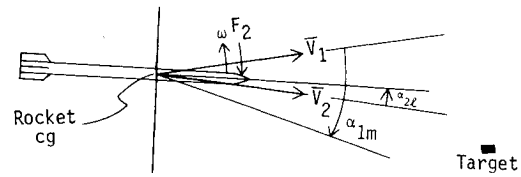

ω = angular velocity
α_{1m} = maximum angle of attack on first swing
$\bar{V}_1$, $\bar{V}_2$ = velocity prior to and after 1st correction
$\alpha_{2\ell}$ = Angle of attack when second correction is made at second laser pulse
$\bar{F}_2$ = second thrust force

Fig. 4 Idealized thruster correction.

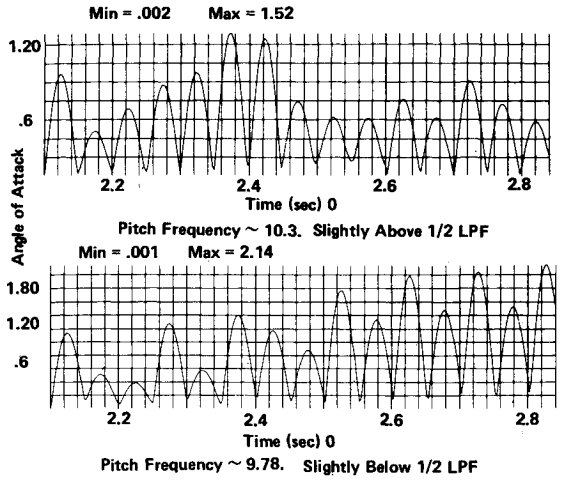

Fig. 5 Angle of attack vs time: two pitch frequencies.

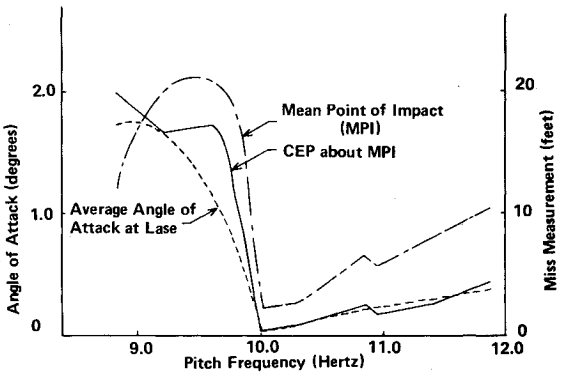

Fig. 6 Average lase angle of attack, mean point of impact, and CEP vs pitch frequency.

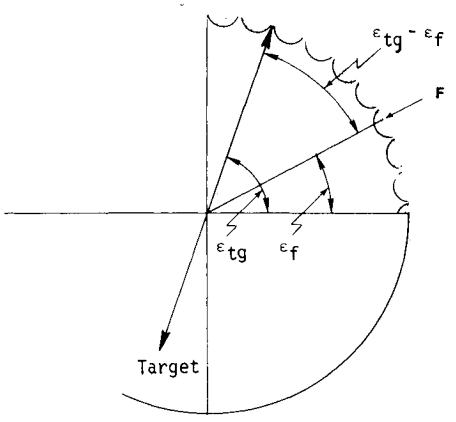

Fig. 7 Thruster correction error.

limited in number and total impulse and therefore limit the correction toward the target. It can be shown simply that the maximum correction toward the target is given by

$$\delta_{rp} = (m+1) R_0 \{ 1 - (T_l/T_f)(m/2) \} \delta_s \quad (8)$$

where δ_s is given by Eq. (7), and m is one less the number of impulses expended prior to impact.

Since the target is detected only to within 90 deg, the correction toward the target will, in general, be in error, and Eq. (8) will give a value too large. This is demonstrated in Fig. 7, where a hypothetical case for one quadrant is shown. The correction for the target image shown is applied at the angle ϵ_f rather than the correct angle ϵ_{tg} (where ϵ_f is the quadrant angle defining the direction of the applied thrust, and ϵ_{tg} is the quadrant angle defining the direction to the target).

For better values for correction to target, the error angle $(\epsilon_{tg} - \epsilon_f)$ of the applied thrust direction should be taken into account. The thrust then will have the following component in the direction toward the target:

$\bar{F}_{tg} = \bar{F} \cos(\epsilon_{tg} - \epsilon_f)$
$\bar{F}_{tg}$ = component of thrust toward the target
$\epsilon_{tg} - \epsilon_f$ = error angle of the applied thrust

It will be assumed that the perpendicular component of the thrust will average to zero, since the thrust is just as likely to be on one side of the target as the other. It is reasonable to assume that a more accurate estimate of the maximum correction toward the target is

$$\delta_{rpq} = \delta_{rp} \cos\{ E[(\epsilon_{tg} - \epsilon_f)^2] \}^{1/2} \quad (9)$$

The expected value of the error angle will depend on the geometry and sequencings of the thrusters and the target image distribution. It is reasonable to assume that the angle position of the target image is a random variable uniformly distributed over the quadrant. In order to simplify the problem, it will be assumed that the thrusters also have a random uniform distribution over a quadrant (that is, no account will be taken of the change in the thruster distribution with thruster depletion). Assume a uniform distribution of ϵ_{tg} and ϵ_f. Also assume that ϵ_{tg} is independent of ϵ_f; then the probability density functions for ϵ_f and ϵ_{tg} are

$$f(\epsilon_{tg}) = f(\epsilon_f) = 1/90;\ 0 \le \epsilon_f \le 90 \text{ deg},\ 0 \le \epsilon_{tg} \le 90 \text{ deg} \quad (10)$$

Using the assumptions that ϵ_{tg} is independent of ϵ_f and normal procedures for evaluating the expected value, it follows that

$$\{ E[(\epsilon_{tg} - \epsilon_f)^2] \}^{1/2} = 37.7 \text{ deg} \quad (11)$$

The six-degree-of-freedom guidance model was used to show the validity of the use of Eq. (9) as a design tool. Accuracy samples were simulated for two configurations, A and B. Configuration B had a higher thruster impulse and slightly greater moment arm than A, giving a larger value for δ_{rpq}. The target array for the simulations had targets at 50 and 100 ft from the unguided impact point. Table 4 shows that for configuration A the CEP value is quite large (11 ft) for targets at 100 ft. This is understood readily, since δ_{rpc} is 84 ft. In configuration B, δ_{rpc} is 108 ft, the targets at 100 ft are accessible, and the CEP comes down to a low value of 1.3 ft.

Trim Misalignment Effect

A misalignment of the body components or tail fins will cause aerodynamic forces and moments on the rocket which result in the rocket trimming out at some angle of attack greater than zero. For a spinning rocket, this trim misalignment causes the rocket's longitudinal axis to perform a lunar type of motion about the velocity vector at an angle of attack (trim angle). For the guidance system being considered, this will result in error correction and premature expenditure of thrusters, giving poor accuracy.

The magnitude of the dynamic trim arm is primarily a function of the trim moment, the physical and aerodynamic characteristics of the missile, and the missile spin. The magnitude of the dynamic trim arm (K_t) is given in Eq. (12). This equation was reduced from Ref. 3. The reduction required the assumption of low spin rate, a simple trim moment given by $QsdC_{m\alpha}\delta_m$, and the elimination of small magnitude terms. A nonrolling missile trims at the static trim angle (δ_m).

$$K_t \simeq \delta_m \left/ \left| -\left(\frac{p}{\omega_l}\right)^2 \left(1 - \frac{I_x}{I_y}\right) + 1 \right| \right. \quad (12)$$

Figure 8 gives the angle of attack of the missile vs the roll rate for three different trim misalignments. The angle of attack is computed from Eq. (12), and the average angle of

Table 4 Accuracy analysis of two configurations with different expected corrections

Configuration	δ_{rpq}[a]	Target set	$\Delta\bar{X}_{ep}$[a]	$\Delta\bar{Y}_e$[a]	$\bar{R}$[a]	$\sigma\Delta X_{ep}$[a]	$\sigma\Delta Y_e$[a]	σ_{cep}[a]
A	84	50 ft	−2.4	0.2	2.4	0.5	0.5	0.6
		100 ft	−1.7	1.8	2.5	7.6	11.4	11.2
		All	−2.2	0.7	2.3	4.4	6.7	6.5
B	108	50 ft	−2.7	−0.3	2.7	1.4	0.5	1.1
		100 ft	−2.0	0.3	2.0	0.5	1.8	1.3
		All	−2.5	−0.1	2.5	1.2	1.1	1.4

[a] Measured in feet.

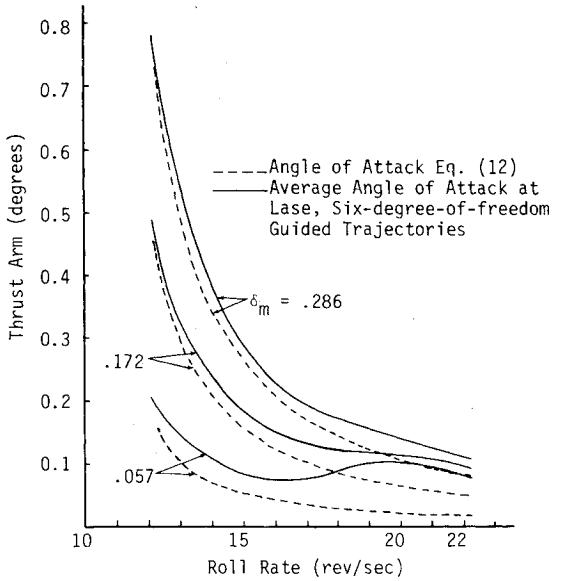

Fig. 8 Angle of attack vs roll rate.

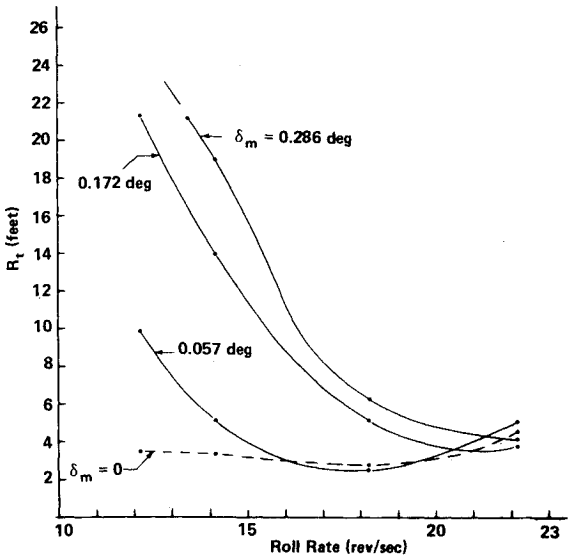

Fig. 9 Total miss distance (R_t) vs missile roll rate.

attack at lase is taken from samples of six-degree-of-freedom guided trajectories for this system. The curves show that the complex guided trajectories have the same form as that given by Eq. (12).

Figure 9 shows that the total miss distance follows the same trend as the angle of attack in regard to missile roll rate. Figure 9 consists of plots of the total miss distance (mean point of impact plus the CEP) vs the missile roll rate. The total miss is also plotted for the missile with no trim misalignment. This analysis indicated that miss distances due to trim misalignment can be reduced to acceptable values by increasing the roll rate to about 1.9 times the pitch frequency.

Summary and Conclusions

It was determined that, to obtain sufficient accuracy for this system, it was necessary to phase the pitch frequency with the laser pulse frequency. The pitch frequency must be slightly greater than one-half the laser pulse frequency. A pitch frequency below one-half the laser pulse frequency results in resonant buildup of the angle of attack and large miss distances. A gradual increase in miss distance occurs as the pitch frequency is increased above one-half the laser pulse frequency. This is due to pitch and laser pulse frequency being out of phase but not in a manner to cause a resonant buildup in angle of attack. The rocket can be designed to accommodate pitch frequency changes resulting from nominal changes in initial launch velocities without a large loss in accuracy.

Approximate formulas were derived to give the maximum expected correction and other useful information for any specified rocket configuration. These formulas can be used in preliminary design to determine if the configuration can correct sufficiently far from the unguided trajectory. The errors due to the quadrant type of corrections are accounted for statistically in the derivation of the formula.

The relation between the accuracy of this system and the trim misalignment was determined. A simple equation (from linear theory) gives the trim angle as a function of trim misalignment, the pitch frequency, and the roll rate. The six-degree-of-freedom guidance program showed that increasing the roll rate (to reduce the trim angle) from 1.2 to 1.8 times the pitch frequency improved the accuracy by a factor of 10.

References

[1] Cobb, K. K., "Design Considerations for an Impulse Corrected, Body Fixed, Laser Guided, Fin Stabilized Rocket," Air Force Armament Lab., AFATL-TR-76-90, Aug. 1976.

[2] Uselton, R. L., "A Wind Tunnel Investigation of Impulse Effects on the Motion of an Impulse Correction Guidance Missile," Arnold Engineering Development Center, AEDC-TR-76-6, Air Force Armament Lab., AFATL-TR-75-164, April 1976.

[3] Murphy, C. H., "Free Flight Motion of Symmetric Missiles," Ballistic Research Lab., Rept. 1216, July 1963.

[4] Uselton, J., "Results of an Air Force Advanced Tactical Rocket Development Program," Arnold Engineering Development Center, AEDC-TR-71-141, Air Force Armament Lab., AFATL-TR-71-73, July 1971.

[5] Groves, A. D., "Handbook on the Use of the Bivariate Normal Distribution in Describing Weapon Accuracy," Ballistic Research Lab., Memo. Rept. 1372, Sept. 1961.